Ultrasound in Med. & Biol., Vol. 35, No. 10, pp. 1756–1760, 2009

0301-5629/09/$–see front matter

ELSEVIER

doi:10.1016/j.ultrasmedbio.2009.05.012

● *Original Contribution*

THE SIZE OF SONOPORATION PORES ON THE CELL MEMBRANE

YUN ZHOU,* RONALD E. KUMON,* JIANMIN CUI,† and CHERI X. DENG*
*Department of Biomedical Engineering, University of Michigan, Ann Arbor, MI, USA
and †Department of Biomedical Engineering, Washington University at St. Louis, MO, USA

(*Received* 13 *April* 2009, *revised* 5 *May* 2009, *in final form* 18 *May* 2009)

Abstract—Sonoporation uses ultrasound (US) to generate transient nonselective pores on the cell membrane and has been exploited as a nonviral intracellular drug and gene delivery strategy. The pore size determines the size of agents that can be delivered into the cytoplasm using the technique. However, measurements of the dynamic, submicron-scale pores have not been readily available. Electron microscopy or atomic force microscopy has been used to gauge pore size but such techniques are intrinsically limited to post-US measurements that may not accurately reveal the relevant information. As previously demonstrated, changes of the transmembrane current (TMC) of a single cell under voltage clamp can be used for monitoring sonoporation in real-time. Because the TMC is related to the diffusion of ions through the pores on the membrane, it can potentially provide information of the pore size generated in sonoporation. Using *Xenopus laevis* oocytes as the model system, the TMC of single cells under voltage clamp was measured in real-time to assess formation of pores on the membrane in sonoporation. The cells were exposed to US (0.2 s, 0.3 MPa, 1.075 MHz) in the presence of Definity™ microbubbles. Experiments were designed to obtain the TMC corresponding to a single pore on the membrane. The size of the pores was estimated from an electro-diffusion model that relates the TMC with pore size from the ion transport through the pores on the membrane. The mean radius of single pores was determined to be 110 nm with standard deviation of 40 nm. This study reports the first results of pore size from the TMC measured using the voltage clamp technique. (E-mail: cxdeng@umich.edu)

Key Words: **Sonoporation, Ultrasound, Nonselective pores, Voltage clamp, *Xenopus laevis* oocyte, Microbubbles, Definity, Electro-diffusion model, Drug delivery, Gene delivery.**

INTRODUCTION

Ultrasound (US)-induced cell membrane porosity, or sonoporation, has shown its unique potential in intracellular drug and gene delivery via generation of nonspecific openings or pores on the cell membrane. It is important to have accurate measurements of the spatial and temporal scales of these pores because they determine the size of molecules or agents that can be efficiently delivered into the cytoplasm using the technique. Scanning electron microscopy (SEM) and atomic force microscopy (AFM) have been employed to obtain information about the pores (Mehier-Humbert et al. 2005; Ross et al. 2002; Schlicher et al. 2006; Zhao et al. 2008). However, such techniques have intrinsic limitations in a sonoporation study. Due to the rapid resealing of the pores (within seconds) in the cell membrane, pores recognized by SEM or other post US assays may not accurately represent practically relevant pore information for delivery. In addition, these techniques are usually time consuming and labor-intensive.

We have previously demonstrated the feasibility of using the voltage clamp technique to monitor the dynamic sonoporation process in real-time (Deng et al. 2004; Zhou et al. 2008a). The inward transmembrane current (TMC) of a single cell under voltage clamp exhibits a rapid increase in amplitude due to US application before recovering to its pre-US level, indicating pore formation and resealing of the pores generated by US exposure (Deng et al. 2004). As the change of TMC is the result of ions flowing through all the transient pores generated on the membrane and, thus, related to the total area of all the pores, the TMC can be used to estimate the size of the pores. The number of pores and the size distribution of pores have to be known to obtain the size of an individual pore. It is hypothesized that with an appropriate model relating the TMC with the radius of pores, a single, reparable pore in the oocyte membranes

Address correspondence to: Cheri X. Deng, Department of Biomedical Engineering, University of Michigan, 2200 Bonisteel Blvd., Ann Arbor, MI 48109–2099, USA. E-mail: cxdeng@umich.edu

produced by acoustic cavitation of microbubbles can be inferred with reasonable accuracy.

To obtain the size of a single pore, sonoporation experiments were conducted under conditions designed to ensure generation of a single pore in the cell membrane with high probability in this study. An electro-diffusion model was developed to relate the radius of a single pore with the TMC so that the size of a single pore was estimated from the recorded TMC. Applicable for quasi-steady state situations, we only consider the maximum pore size from the maximum TMC in this study, while the radius as a function of time can be derived from the time-dependent TMC values.

MATERIALS AND METHODS

Cell preparation

Collegenase-treated and defolliculated *Xenopus laevis* oocytes were used in this study. They were prepared following a protocol approved by our Institutional Animal Care and Use Committee (Deng et al. 2004; Zhou et al. 2008b). The oocytes were used immediately in experiments or stored in ND96 solution (96 mM NaCl, 2 mM KCl, 1 mM $MgCl_2$, 1.8 mM $CaCl_2$, 5 mM HEPES, pH = 7.6) at 18 °C for 1 or 2 days before use.

Sonoporation

During each experiment, a single oocyte (~1.1 mm diameter) was housed in a 35 mm polystyrene Petri dish (BD Biosciences, San Jose, CA, USA) containing 4 mL ND96 solution with Definity microbubbles (Lantheus Medical Imaging, N. Billerica, MA, USA) at a concentration of 6×10^3/mL to facilitate sonoporation (Deng et al. 2004; Zhou et al. 2008b). The actual microbubble concentration was confirmed by counting the bubbles with a hemocytometer. Tone-burst US exposures (center frequency 1.075 MHz, duration 0.2 s, peak negative pressure 0.3 MPa) were generated using an planar, circular piezoelectric US transducer (Piezo Technologies, Indianapolis, IN, USA) driven by a waveform generator (33250A, Agilent Technologies, Palo Alto, CA, USA) and a RF power amplifier (75A250, Amplifier Research, Souderton, PA, USA). The Petri dish was tested to have minimal effect (>95% transmission) on the transmitting US. Fresh solution with Definity microbubbles was used after each US application (with or without TMC change) and each oocyte was used for only one detected TMC change.

Electrophysiological measurements

Microelectrodes connected to a voltage clamp amplifier (Dagan CA-1B, Dagan Corporation, Minneapolis, MN, USA) (Stuhmer 1998) were inserted into the oocyte membrane to measure the TMC when the membrane potential was clamped at −50 mV during recordings. Recording of TMC was synchronized with US application using the voltage clamp trigger signals to allow continuous measurement before, during and after US (Deng et al. 2004) at a sampling rate of 1.0 kHz. The whole cell clamp configuration measures the ion movement through all of the pores generated on the cell membrane.

Experimental design for single-pore generation

We assume that cavitation (*i.e.*, US induced bubble oscillation and collapse) (Zhou et al. 2008a) provides the primary mechanism for sonoporation in this study. Previous work has suggested that the microbubbles, which facilitate cavitation must be close to the cell membrane to be effective in generating pores (Guzman et al. 2003). Below we describe the design of experimental condition to ensure generation of a single pore in our study.

The number of homogeneously distributed microbubbles within a given volume surrounding the cell follows a Poisson distribution. Assuming that each pore is generated by one bubble, the probability of having N pores (by N porating bubbles) on the membrane is described by a Poisson distribution (Walpole et al. 2007)

$$f(N;\lambda)=\lambda^N e^{-\lambda}/N!, \tag{1}$$

where λ is the mean value of the number of pores. The probability of having no pores is described by $p_0 = f(0;\lambda)$ and $p_1 = f(1;\lambda)$ describes the probability of having one pore. Thus the probability of having at least one pore ($N \geq 1$) is

$$p_{pore}=1-p_0=1-f(0;\lambda). \tag{2}$$

Furthermore, the conditional probability of having one pore whenever poration occurs is

$$p_{1|pore}=p_1/p_{pore}=f(1;\lambda)/[1-f(0;\lambda)]. \tag{3}$$

Therefore, generation of a single pore can be ensured in experiment if a high level (*e.g.*, >95%) of $p_{1|pore}$ is maintained.

On the other hand, p_{pore} can be calculated as the ratio of the number of the experimental tests in which a change of TMC is measured (n_{curr}) over the total number of tests n_{tot}, or n_{curr}/n_{tot}. Equation (2) allows an experimental determination of λ, or the mean of the Poisson distribution in eqn (1) and $p_{1|pore}$ is then determined from eqn (3). Obviously, decreasing the microbubble concentration reduces p_{pore} and the likelihood of generating only one pore ($p_{1|pore}$) increases consequently. Single pore sonoporation can be achieved by using sufficiently low bubble concentration to ensure an appropriately low value of p_{pore}, thus, high value of $p_{1|pore}$.

Model

The change of the TMC during sonoporation results from ion transport through the nonspecific pore(s) and is driven by the ion concentration and electrical potential gradient across the membrane. Of all the ions present, significant contribution to the TMC only comes from Na^+, K^+ and Cl^- (Costa et al. 1989). The current density (current per unit area) of the kth ion is calculated via the Goldman-Hodgkin-Katz (GHK) current equation (Hille 2001):

$$i_k = z_k F P_k U_k \left(c_k^{in} \exp U_k - c_k^{ex}\right) / (\exp U_k - 1), \qquad (4)$$

where $U_k = z_k FV/RT$; z_k are the ion valencies; F, the Faraday constant; V, the membrane potential in relation to the exterior surface of the membrane; R, the ideal gas constant, T, the temperature; $P_k = D_k K_k / h$, the ion permeabilities; D_k, the ion diffusion coefficients; K_k, the ion partition coefficients; c_k^{in} and c_k^{ex}, the intra- and extracellular ion concentrations; and h, the membrane thickness. If i_{tot} is the total current density, then the total TMC is $I = i_{tot}(\pi r^2)$ where r is the (effective) radius of the pore and, hence,

$$r = \sqrt{I/(\pi i_{tot})}. \qquad (5)$$

Figure 1 shows the pore radius as a function of pore TMC using eqns (4) and (5) with P_k^{pore}. Table 1 lists the parameters used in calculation in the model. In addition, $V = -50$ mV, $h = 5$ nm (DeBruin and Krassowska 1999) and $T = 293$ K. In the case of poration, it is assumed $K_k = 1$ (no membrane in the pore) and, hence, $P_k^{pore} = D_k/h$.

RESULTS AND DISCUSSION

Typical TMC measurements from control and test group experiments are shown in Figure 2. The start and end of the ultrasound application is indicated by the vertical dotted lines. Figure 2A shows a typical control data with ultrasound application without microbubbles in the extracellular solution. Similarly, control experiments with no ultrasound (with and without microbubbles) exhibited no TMC change (data not shown). Figure 2B shows the result of a typical test experiment with ultrasound applied in the presence of microbubbles. The change of TMC was defined as the difference between the mean TMC before ultrasound was applied and the maximum amplitude of (inward) TMC measured. The TMC usually reaches its maximum value during or shortly after the end of the ultrasound pulse and then gradually recovers to its pre-ultrasound value over 5 to 20 s. For this study, the maximum TMC change was of primary interest as it corresponded to the maximum pore size.

A total of 579 (n_{tot}) tests were conducted under identical conditions for measuring TMC in sonoporation.

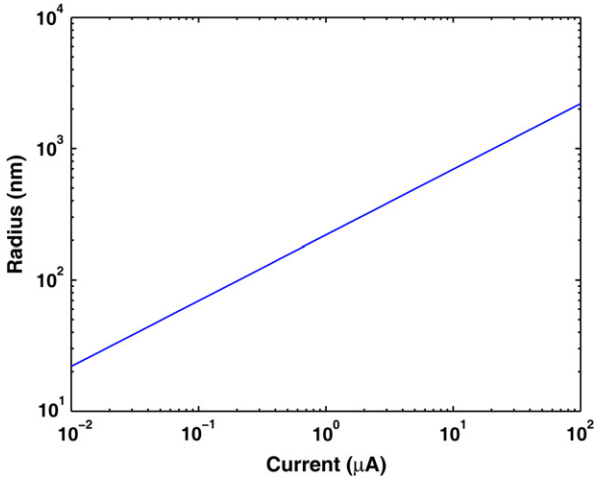

Fig. 1. Maximum pore radius as a function of the maximum transmembrane current amplitude computed using eqns (4) and (5) with P_k^{pore}.

Of these tests, TMC change was observed in 54 (n_{curr}) tests. Therefore, $p_{pore} = 54/579 = 0.0933$, $\lambda = 0.0979$ from eqn (2) and $p_{1|pore} = 95.2\%$ from eqn (3). Thus, the measured TMC in these experiments very likely resulted from only a single pore on the membrane during sonoporation. Figure 3A shows the histogram of the maximum amplitude of the TMC measured from the set of experimental tests described above. The mean TMC is 261.4 nA (median 199.0 nA) with a standard deviation (SD) of 196.9 nA. The histogram is shown with a gamma distribution (shape = 1.76, scaling = 0.148) with the same mean, variance and area as the measured histogram. Figure 3B shows the corresponding distribution of pore sizes computing via eqns (4) and (5) (cf. Fig. 1). The mean radius of single pores is 110 nm (median 98 nm) with SD of 40 nm. The curve is the size distribution corresponding to the gamma distribution in Figure 3A transformed using eqn (5) by the standard method (Walpole et al. 2007).

Our estimates of pore size are in the same range as the previous studies obtained by SEM, which was reported to be ~50–75 nm (Mehier-Humbert et al. 2005), ~500 nm (Schlicher et al. 2006) and 500–2500 nm (Zhao et al. 2008) in radius. One advantage of our approach is the

Table 1. Model parameters

Ion	c_k^{ex} [mM]*	c_k^{in} [mM]†	D_k [m²/s]‡	P_k [m/s]†	P_k^{pore} [m/s]§
Na^+	96	10.1	1.33×10^{-9}	3.75×10^{-10}	0.266
K^+	2	109.5	1.96×10^{-9}	9.55×10^{-10}	0.392
Cl^-	100	37.7	2.03×10^{-9}	3.40×10^{-10}	0.406

*For ND96; †From Costa et al (1989); ‡From Cussler (1997); §Using D_k from Cussler (1997) with $h = 5$ nm.

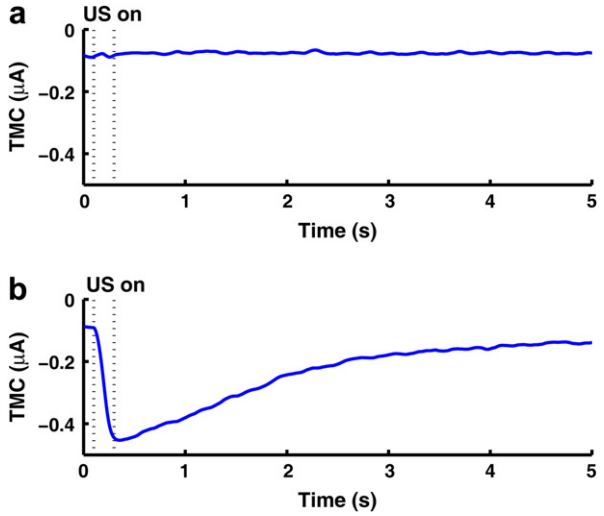

Fig. 2. (a) Typical transmembrane current (TMC) for control experiment with ultrasound application but no microbubbles introduced. (b) Typical TMC for test experiment with ultrasound application with microbubbles introduced.

ability to estimate more readily the size of rapidly-closing or completely-closed pores without necessarily performing post-US assays. The effective range for a microbubble to induce sonoporation can also be estimated. With a spherical oocyte of diameter 1.1 mm, there is an average of only one bubble in a shell volume of a thickness $\Delta h_{sb} = 44\ \mu$m around the oocyte at bubble concentration of 6×10^3/mL. Pores occur only 9.33% of the time in our experiments, suggesting an effective range $\Delta h_{pore} = 4.1\ \mu$m.

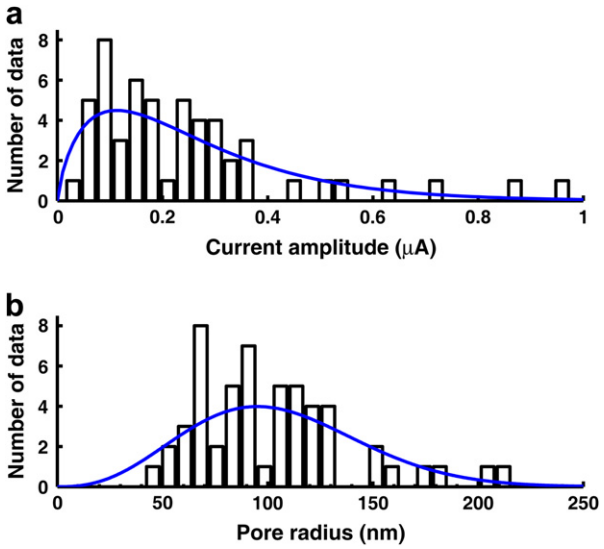

Fig. 3. (a) Measured histogram of the maximum change in typical transmembrane current (TMC) from single pore data along with fitted curve. Bin size = 0.03 μA, sample size $n = 54$. (b) Corresponding calculated histogram of maximum pore radii based on Figure 1. Bin size = 7.5 nm.

Sonoporation is believed to create on the cell membrane non-selective pores, wherein the potential gradient and ion concentration are generally unknown. It is thus difficult to assess the strict applicability of the GHK current equation, which assumes a linear potential gradient across the membrane, no interaction between ions, no convection and steady state conditions. Particularly if a large pore is created (diameter >> membrane thickness), it is difficult to know if the potential gradient is linear without detailed numerical simulations. Nevertheless, the GHK current equation should be applicable on a quasi-static basis because the characteristic ion diffusion time between the intra- to extracellular spaces is typically very fast ($\sim\mu$s), while the TMC in sonoporation typically recovers in ~10–20 s (Deng et al. 2004; Zhou et al. 2008b). Although convection due to bubble collapse may occur, its effect will also be very fast ($\sim\mu$s), after which electro-diffusion should be the dominant transport mechanism.

It is possible that US could enhance permeation of the membrane without creating large physical pores. In this case, the effect of sonoporation could be modeled by using an effective or equivalent permeability for the whole cell membrane. This effective permeability will have a value between the normal, pre-US permeabilities P_k and the pore permeabilities P_k^{pore} (where $K_k = 1$, indicating no membrane) listed in Table 1, as it is essentially the average of the pore permeability over the whole membrane. Even without precise knowledge of the physical picture or mechanisms responsible for the enhanced permeability resulted from US exposure, the estimation of pore size obtained using our method will be the upper bound, if consideration is given to the possibility of other sources of contribution to the measured TMC change.

In conclusion, this study reports results of pore size obtained from the TMC measured using the voltage clamp technique in single-pore sonoporation experiments. The TMC measurements were related to pore size using the GHK current equation, providing a simple approach to estimate pore size in sonoporation. The estimates of pore size computed from the TMC measurements are consistent with the proposed hypothesis and in the same range as previous studies using SEM (Mehier-Humbert et al. 2005; Schlicher et al. 2006; Zhao et al. 2008).

Acknowledgements—This work was supported in part by the National Institutes of Health (R01CA116592 to C. X. Deng).

REFERENCES

Costa PF, Emilio MG, Fernandes PL, Ferreira HG, Ferreira KG. Determination of ionic permeability coefficients of the plasma membrane of *Xenopus laevis* oocytes under voltage clamp. J Physiol 1989;413: 199–211.

Cussler EL. Diffusion: Mass transfer in fluid systems. New York, NY: Cambridge University Press; 1997.

DeBruin KA, Krassowska W. Modeling electroporation in a single cell. I. Effects of field strength and rest potential. Biophys J 1999;77: 1213–1224.

Deng CX, Sieling F, Pan H, Cui J. Ultrasound-induced cell membrane porosity. Ultrasound Med Biol 2004;30:519–526.

Guzman HR, McNamara AJ, Nguyen DX, Prausnitz MR. Bioeffects caused by changes in acoustic cavitation bubble density and cell concentration: A unified explanation based on cell-to-bubble ratio and blast radius. Ultrasound Med Biol 2003;29:1211–1222.

Hille B. Ion channels of excitable membranes. Sunderland, MA: Sinauer Associates, Inc.; 2001.

Mehier-Humbert S, Bettinger T, Yan F, Guy RH. Plasma membrane poration induced by ultrasound exposure: Implication for drug delivery. J Control Release 2005;104:213–222.

Ross JP, Cai X, Chiu JF, Yang J, Wu J. Optical and atomic force microscopic studies on sonoporation. J Acoust Soc Am 2002;111: 1161–1164.

Schlicher RK, Radhakrishna H, Tolentino TP, Apkarian RP, Zarnitsyn V, Prausnitz MR. Mechanism of intracellular delivery by acoustic cavitation. Ultrasound Med Biol 2006;32:915–924.

Stuhmer W. Electrophysiologic recordings from *Xenopus* oocytes. Methods Enzymol 1998;293:280–300.

Walpole RE, Myers RH, Myers SL, Ye K. Probability and statistics for engineers and scientists. Upper Saddle River, NJ: Pearson Prentice Hall; 2007.

Zhao YZ, Luo YK, Lu CT, Xu JF, Tang J, Zhang M, Zhang Y, Liang HD. Phospholipids-based microbubbles sonoporation pore size and reseal of cell membrane cultured *in vitro*. J Drug Target 2008;16:18–25.

Zhou Y, Cui J, Deng CX. Dynamics of sonoporation correlated with acoustic cavitation activities. Biophys J 2008a;94:L51–L53.

Zhou Y, Shi J, Cui J, Deng CX. Effects of extracellular calcium on cell membrane resealing in sonoporation. J Control Release 2008b;126: 34–43.